

Template-free electrodeposition of multicomponent metal nanoparticles for region-specific growth of interposed carbon nanotube micropatterns

This article has been downloaded from IOPscience. Please scroll down to see the full text article.

2005 Nanotechnology 16 2111

(<http://iopscience.iop.org/0957-4484/16/10/023>)

View [the table of contents for this issue](#), or go to the [journal homepage](#) for more

Download details:

IP Address: 129.22.124.187

The article was downloaded on 02/04/2012 at 14:29

Please note that [terms and conditions apply](#).

Template-free electrodeposition of multicomponent metal nanoparticles for region-specific growth of interposed carbon nanotube micropatterns

Lingchuan Li and Liming Dai¹

Department of Chemical and Materials Engineering, School of Engineering and UDRI,
University of Dayton, 300 College Park, Dayton, OH 45469-0240, USA

E-mail: ldai@udayton.edu

Received 19 May 2005, in final form 27 June 2005

Published 9 August 2005

Online at stacks.iop.org/Nano/16/2111

Abstract

We have demonstrated that multicomponent carbon nanotube micropatterns, in which different nanotubes are interposed in an intimate fashion, can be prepared by pyrolytic growth of carbon nanotubes on interposed micropatterns of different metal nanoparticles generated by template-free pulsed electrodeposition of metal-containing salts onto a photolithographically prepatterned conductive surface at different peak potentials. The resultant multicomponent interposed carbon nanotube micropatterns should have important implications for the construction of multicomponent and multifunctional nanomaterials and nanodevices based on carbon nanotubes for a wide range of potential applications.

(Some figures in this article are in colour only in the electronic version)

1. Introduction

With the recent significant advances in nanoscience and nanotechnology, various nanostructured metals and metal alloys have been prepared for a wide range of potential applications. Examples include the use of metal nanoparticles as advanced catalysts and metal nanowires as efficient electron emitters [1, 2]. In particular, a large number of techniques, including the vapour deposition of metal thin films coupled with annealing in a reducing atmosphere [3–7], wet deposition of dilute solutions of metal salts followed by calcinations and annealing in reducing atmosphere [8–11], direct inclusion of metal nanoparticles in colloid suspension [12–19] or sol–gel systems [20, 21], and plasma etching or ion bombardment of metallic substrates [22, 23], have been devised for preparing metal nanocatalysts on substrates for carbon nanotube growth. Although the electroplating of metals on conductive substrates has a long history in industrial applications, only a few recent studies involve the use of electrodeposited metals, mainly in the

nanopores of alumina template membranes, to produce metal nanoparticles for the growth of carbon nanotubes [24–26]. In these cases, a rather tedious post-synthesis process is often required to remove the template to produce pure carbon nanotubes [27].

On the other hand, carbon nanotubes have been demonstrated to be useful in many microscale or nanoscale electronic and photonic devices [28]. The ability to manipulate them for heterogeneous integration on a micrometre to nanometre scale is of paramount importance to both fundamental characterization and potential applications of carbon nanotubes in various advanced optoelectronic devices [28, 29]. In this context, we have developed microfabrication methods for micropatterning of carbon nanotubes with a submicrometre resolution [30–32]. Following our earlier work on the microfabrication of carbon nanotubes, we have recently carried out the *template-free* electrodeposition of cobalt (nickel) nanoparticles by applying an AC voltage across an aluminium working electrode and graphite (nickel foil) counter-electrode in a two-electrode electrochemical cell containing an aqueous solution of 0.4 M H₃BO₃ and 0.3 M CoSO₄ (0.3 M NiSO₄).

¹ Author to whom any correspondence should be addressed.

The resultant metal nanoparticles with a nanometre-scale size, together with the ease with which multicomponent interposed metal nanoparticle micropatterns could be prepared by a region-specific template-free electroplating, prompt us to grow interposed multicomponent micropatterns of different carbon nanotubes from the interposed micropatterns of different metal nanoparticles. Here, we report this simple, but very effective, *template-free* electroplating method for *region-specific* deposition of cobalt and nickel nanoparticles for patterned growth of carbon nanotubes. The resulting carbon nanotube micropatterns in which multicomponents are interposed in a controllable fashion should be of significance for many nanotube-based multifunctional systems, such as sensor chips and multifunctional optoelectronic devices [33].

2. Experimental details

2.1. Materials and characterization

Aluminium foils were cut into pieces of 12 mm × 60 mm as the electrodes. H_3BO_3 , NiSO_4 and CoSO_4 were all analytical grade, purchased from commercial sources and used without further purification. Positive photoresist AZ 3312 and the corresponding AZ 300 MIF developer were supplied by Clariant Corporation. A medium pressure mercury UV lamp and TEM copper grids of both 200 and 600 meshes were used as the UV light and photomask, respectively, for photopatterning. Scanning electron microscopic (SEM) images were recorded on a Hitachi S-2150 SEM unit and a Hitachi S-900 field emission-type SEM unit. Atomic force microscope (AFM) images were taken with a Digital Instruments AFM (Veeco Metrology), using the tapping mode.

2.2. Patterned and nonpatterned electrodepositions

Prior to the electrodeposition, the aluminium surface was cleaned in an aqueous solution of chromic acid (2 wt%), phosphoric acid (6 wt%) and hydrofluoric acid (0.001 wt%). The aluminium electrodes were then electropolished in a mixture of perchloric acid and alcohol; this was followed by electrodeposition of nickel and cobalt nanoparticles in aqueous solutions of 0.4 M H_3BO_3 /0.3 M NiSO_4 and 0.4 M H_3BO_3 /0.3 M CoSO_4 , respectively. Figure 1 shows the steps of the patterned electrodeposition of nickel and cobalt nanoparticles. Prior to the patterned electrodeposition of metal nanoparticles, a thin layer of positive photoresist (AZ 3312 from Clariant Corporation) was spin-cast on the electropolished aluminium surface; this was followed by drying in an oven at 80 °C. Upon UV exposure from a medium pressure mercury lamp through a TEM grid as the photomask, the photoresist film in the exposed regions was rendered soluble in AZ 300 MIF developer purchased from the same company. Cobalt nanoparticles were then electrochemically deposited into the photoresist-free areas within the patterned photoresist structure under an alternating potential (60 Hz) of 6.5 V with a graphite rod counter-electrode in an aqueous solution of 0.4 M H_3BO_3 and 0.3 M CoSO_4 for 20 s. The newly formed cobalt nanoparticles were then stabilized and preserved by immersing the electrodeposited sample into a 5% potassium dichromate solution. Subsequent washing of the

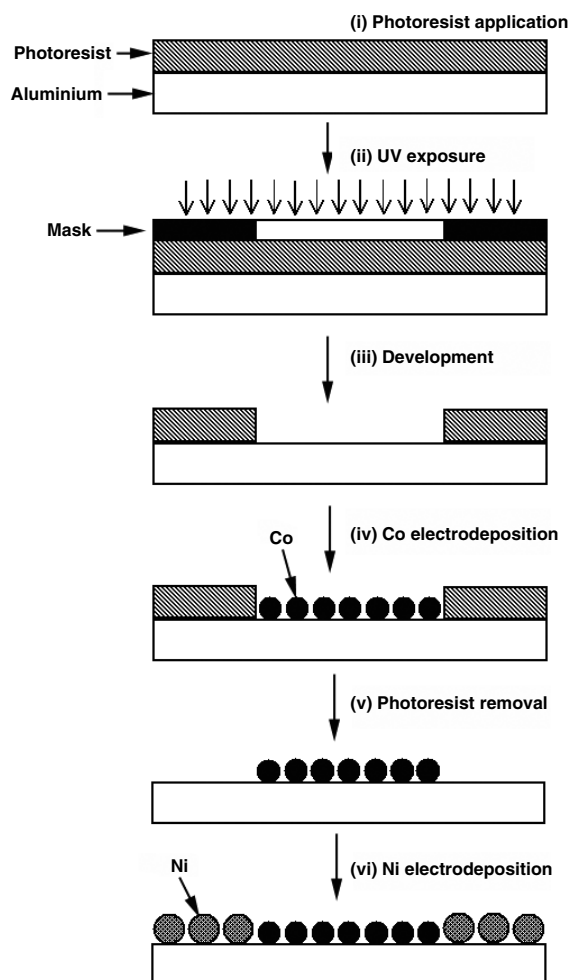


Figure 1. Schematic representation of the region-specific electrodeposition of cobalt and nickel nanoparticles.

cobalt-deposited electrode with flowing water and anhydrous acetone removed the resist that was not exposed to the UV light to regenerate the underlying aluminium surface. After being cleaned again by immersing in a dilute solution of sodium hydroxide and potassium dichromate for a few seconds this time, the resulting electrode prepatterned with cobalt nanoparticles was then used for electrodeposition of nickel nanoparticles at 4.0 V with the alternating power and a nickel foil counter-electrode in an aqueous solution of 0.4 M H_3BO_3 and 0.3 M NiSO_4 for 1 min. As cobalt and nickel nanoparticles were electrodeposited under two different voltages, the high voltage (AC 6.5 V) applied during the cobalt deposition could lead to the formation of a relatively thick charge barrier layer by electro-oxidation of aluminium at the negative half-cycle of the alternating potential, which can act as an effective insulating coating at the relatively low voltage required for the nickel deposition (AC 4.0 V) to avoid the formation of nickel nanoparticles over the cobalt-covered areas. As we shall see later, a desired particle size and packing density for nanotube growth make 20 s and 1 min the electrodeposition times of choice for Co and Ni, respectively.

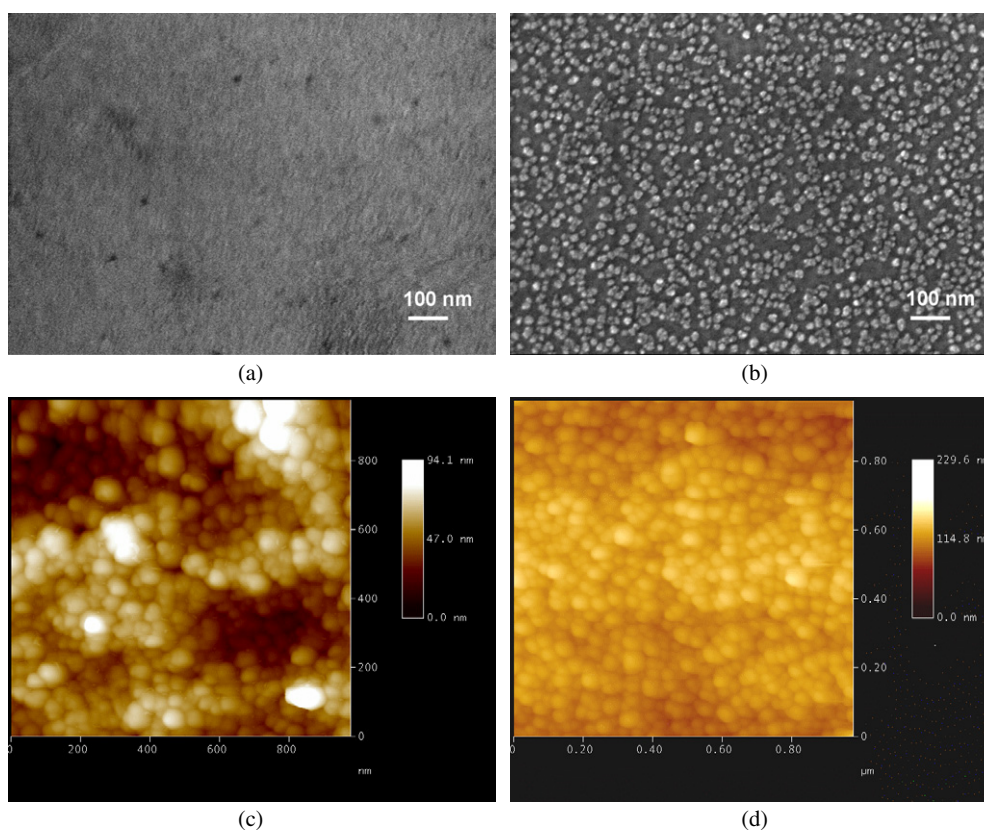


Figure 2. SEM images of (a) an aluminium surface after electropolishing (see section 2), (b) after the template-free electrodeposition of nickel particles at 4.0 V for 5 s; AFM images of (c) the nickel nanoparticles produced by the template-free electrodeposition at 4.0 V for 1 min (scanning area: $1 \mu\text{m} \times 1 \mu\text{m}$; height bar: 94.1 nm), and (d) cobalt nanoparticles produced by the template-free electrodeposition at 6.5 V for 15 s (scanning area: $1 \mu\text{m} \times 1 \mu\text{m}$; height bar: 229.6 nm).

2.3. Carbon nanotube growth

Carbon nanotubes were grown on the Co/Ni-deposited aluminium substrates by pyrolysis of acetylene under H_2/Ar in a quartz tube furnace at 630°C [24]. Prior to the introduction of acetylene as the carbon source for the carbon nanotube growth, the substrates were heated up to 630°C at a preprogrammed heating rate of $50^\circ\text{C min}^{-1}$ and annealed at this temperature for 30 min under hydrogen and argon flow to reduce the catalytic particles to pure metallic form in the quartz tube furnace.

3. Results and discussion

In a typical experiment, we carried out the *template-free* electrodeposition of cobalt (nickel) nanoparticles by applying an AC voltage across an aluminium working electrode and graphite (nickel foil) counter-electrode in a two-electrode electrochemical cell containing an aqueous solution of 0.4 M H_3BO_3 and 0.3 M CoSO_4 (0.3 M NiSO_4). Aluminium foils were chosen for the working electrode because nanoporous membranes can be prepared from the same material by anodizing for template electrodeposition of metal nanoparticles. If necessary, metal nanoparticles prepared by the template electrodeposition can be used as references for comparing with their template-free counterparts.

Figures 2(a) and (b) show typical SEM images for the aluminium surface before and after the template-free

electrodeposition of nickel nanoparticles at 4.0 V for 5 s. As can be seen, particles thus prepared had an average diameter around 20 nm. A longer electrodeposition time caused an increase in the particle packing density and particle diameter.

Figures 2(c) and (d) show typical atomic force microscopy, AFM, images for the Ni and Co nanoparticles electrodeposited without a template at 4.0 V for 1 min and 6.5 V for 15 s, respectively. In both of the AFM images, a homogeneous coverage of spherical nanoparticles with a diameter of about 50 nm is clearly evident. As can be seen in figure 2(c), nickel nanoparticles were even deposited into the pits or small holes which were formed by removal of impurities from the aluminium surface through electropolishing.

The mechanism for nanoparticle formation by *template-free* electroplating is consistent with a pulsed electrodeposition process, in which we used sine wave voltages having a half of the wave period of 8.3 ms (60 Hz) and peak potentials of $-(2)^{1/2} \times 4 = -5.7$ V for nickel and $-(2)^{1/2} \times 6.5 = -9.2$ V for cobalt deposition during the negative half-circle. A pulse potential, which spans a very short time (typically, ms) but at a much higher voltage than that used in conventional direct current electrodeposition, can facilitate the instant formation of small nuclei for the growth of the metal nanoparticles by the *template-free* electrodeposition. The growth of the metal nanoparticles during the high frequency (60 Hz) pulsed electrodeposition process studied here is most probably controlled by diffusion of the electrolytes from the

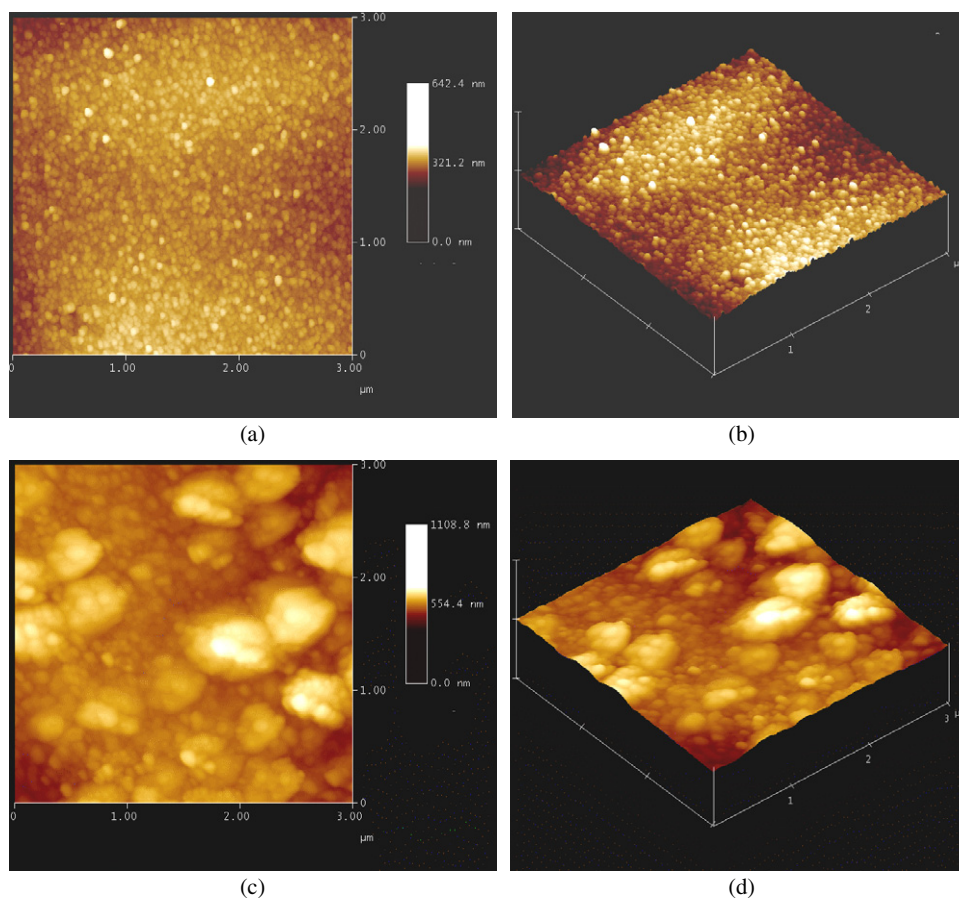


Figure 3. AFM images of (a) the nickel nanoparticles electrodeposited for 5 s after having been heated up to 630 °C in Ar/H₂ for 1 min (scanning area: 3 μm × 3 μm; height bar: 642.4 nm), and (b) as for (a), but the surface view (scanning area: 3 μm × 3 μm); (c) the nickel nanoparticles electrodeposited for 5 min after having been heated up to 630 °C in Ar/H₂ for 1 min (scanning area: 3 μm × 3 μm; height bar: 1108.8 nm), and (d) as for (c), but the surface view (scanning area: 3 μm × 3 μm).

bulk solution to the electrode/solution interface, especially at the early stages of the electrodeposition. Under diffusion control, small particles could grow faster than larger particles at any given time due to an enhanced metal ion supply associated with the relatively high surface-to-volume ratio. Owing to the short pulse period for diffusion of the metal ions from the bulk solution to the electrode, the local concentration of metal ions near to the electrode/solution interface could be constantly too low to support the formation of any abnormally large particle(s). Consequently, all of the nanoparticles produced by the template-free electrodeposition possess a uniform diameter (figure 2)—much like those monodispersed structures produced in a confined space by the template synthesis involving alumina membranes. As can be seen in figure 2, however, the particle size can be regulated within a certain range by controlling conditions for the template-free electrodeposition (e.g. pulse wave width and duration, peak potential).

The above-observed metal nanoparticles having a well-defined diameter, together with the ease with which the multicomponent interposed micropatterns of different metal nanoparticles could be prepared by a region-specific template-free electroplating method developed in this study (*vide infra*), suggests a wide range of potential applications for the resultant metal nanoparticles, especially for (multicomponent)

patterned/nonpatterned growth of carbon nanotubes. To demonstrate the feasibility for growing carbon nanotubes from the template-free electrodeposited metal nanoparticles at a high temperature (e.g. 630 °C), the possible effects of heating on the metal nanoparticles were investigated. Figures 3(a) and (c) show AFM images of the nickel particles electrodeposited for 5 s and 5 min with subsequent heating at 630 °C in Ar/H₂ for 1 min. Also included in the figures are the corresponding surface views (i.e. figures 3(b) and (d)).

Comparison of figure 3(a) with figure 2(b) indicates that no obvious thermally induced aggregation was observed for the nickel nanoparticles generated from the electrodeposition for 5 s after having been heated up to 630 °C in Ar/H₂ for 1 min. In contrast, large particles having diameters of several hundred nanometres were seen for the nickel nanoparticles electrodeposited for 5 min upon heating under the same conditions (figure 3(c)). The newly formed large particles apparently resulted from the thermally induced aggregation of small nanoparticles, as the individual small particles can still be clearly identified around the large entities. Similar thermally induced aggregation was also observed for cobalt nanoparticles produced by template-free electrodeposition for about 20 s, which shows an AFM image similar to figure 2(d) before the heating.

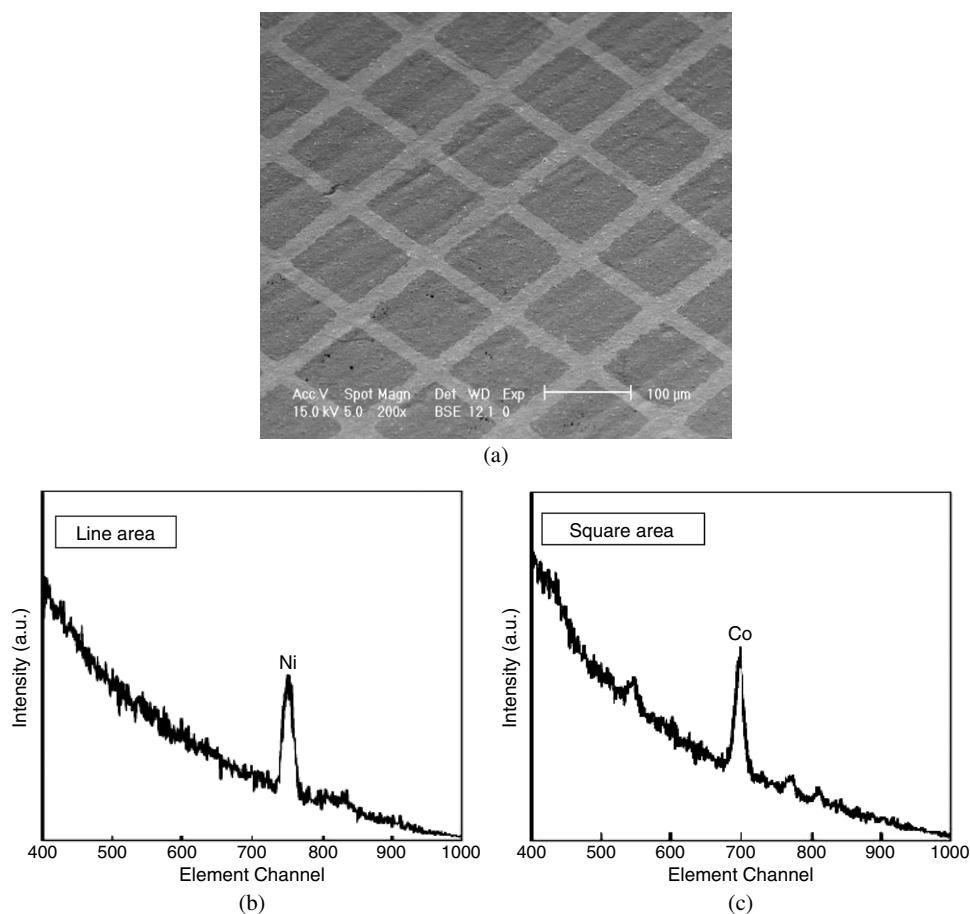


Figure 4. (a) Backscattering electron image of the aluminium surface electrodeposited with the catalytic nanoparticles in patterned format. The darker square area was electrodeposited with cobalt while the light line area was covered with nickel, and ((b), (c)) EDS spectra taken from the line and square areas in (a), respectively.

The absence of thermally induced aggregation for those particles electrodeposited within a relatively short period of deposition time is attributable to the weak interparticle interaction due to a low surface packing density of the particles formed at an initial stage of the electrodeposition process. These results indicate that there is considerable room for regulating diameters of the nanoparticles, and hence the structure of carbon nanotubes subsequently formed, by a simple thermal treatment.

In view of the fact that carbon nanotubes can be grown on both nickel and cobalt nanoparticles [34], we proceeded to prepare interposed multicomponent micropatterns by co-electrodeposition of nickel and cobalt nanoparticles in a region-specific fashion at different reduction potentials (see section 2), and then used the aluminium substrate prepatterned with the nickel and cobalt nanoparticles for region-specific growth of interposed carbon nanotube micropatterns by pyrolysis of acetylene under H_2/Ar at $630^\circ C$. The region-specific electrodeposition was confirmed by the SEM image shown in figure 4(a) recorded with a backscattering electron detector. The corresponding EDS (energy dispersive spectroscopy) profiles given in figures 4(b) and (c) clearly show that nickel and cobalt nanoparticles were deposited within the line and square areas, respectively. No electrodeposition of nickel from an aqueous solution of $0.4 M H_3BO_3$ and $0.3 M NiSO_4$ was

observed at AC $4.0 V$ in the control experiment, in which the aluminium surface was subjected to a peak potential of AC $6.5 V$ in an aqueous solution of $0.4 M H_3BO_3$ prior to the nickel deposition. Similarly, an aluminium substrate with cobalt nanoparticles electrodeposited from the cobalt deposition bath at AC $6.5 V$ was found to not support the electrodeposition of nickel from an aqueous solution of $0.4 M H_3BO_3$ and $0.3 M NiSO_4$ at $4.0 V$ even after removal of the cobalt nanoparticles by dissolving in an aqueous solution of $0.1 M H_2SO_4$. These observations do indeed indicate that a layer of aluminium oxide could have developed at the relatively high voltage of AC $6.5 V$ and acted as a barrier to nickel deposition at AC $4.0 V$.

The resultant aluminium surface covered with the interposed micropatterns of cobalt and nickel nanoparticles was finally used for patterned growth of carbon nanotubes by pyrolysis of acetylene under H_2/Ar in a quartz tube furnace at $630^\circ C$. Figure 5(a) shows a typical SEM image for the resulting carbon nanotube micropatterns, which is a close replication of figure 4(a). Close inspection of figure 5(a) in both the square and line regions clearly shows carbon nanotubes of different structures (figures 5(b) and (c)) grown from both the cobalt and nickel nanoparticles in an interposed fashion, though the nanotube quality has not yet been optimized. The mushroom-like appearance seen in the square regions of figure 5(a) can be attributed to the

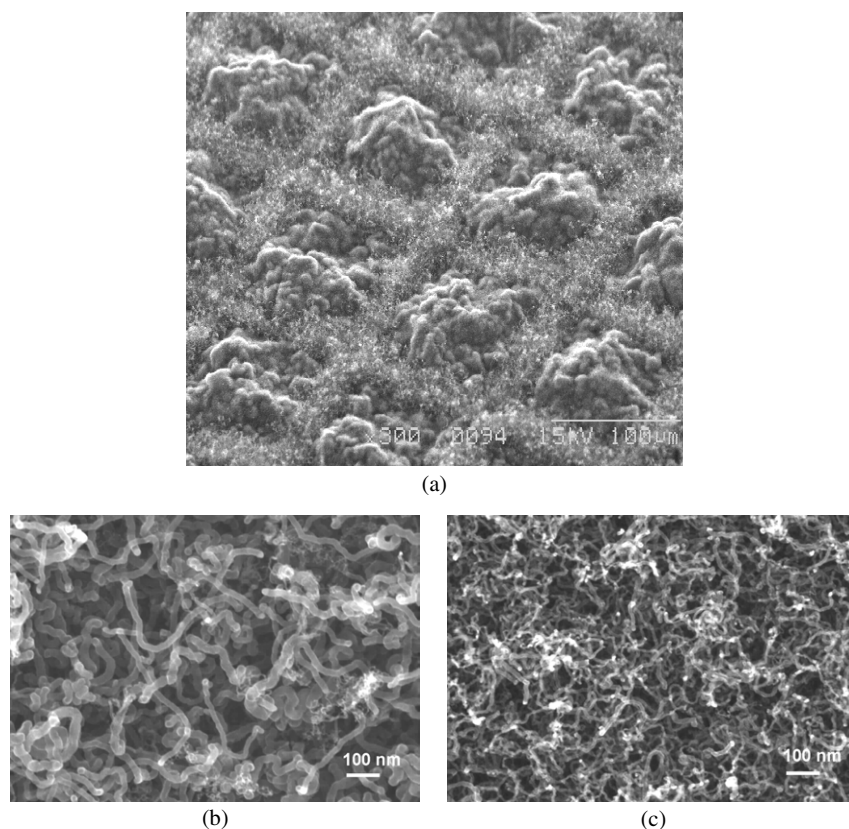


Figure 5. SEM images of the carbon nanotubes grown over the surface electrodeposited with (a) the interposed catalytic nanoparticles, (b) nickel nanoparticles and (c) cobalt nanoparticles taken from the line and square areas, respectively, in (a) under higher magnifications.

annealing-induced aggregation of cobalt nanoparticles during the nanotube growth process, as discussed earlier. As there was no thermally induced aggregation for Ni nanoparticles electrodeposited for 1 min (figure 3), no mushroom-like appearance was observed for carbon nanotubes grown from Ni nanoparticles in the line regions (figure 5(a)).

4. Conclusions

In summary, we have demonstrated that metal nanoparticles can be produced by template-free pulsed electrodeposition of metal-containing salts onto a conductive surface using alternating potentials. This, coupled with photolithographic patterning methods, enabled us to prepare multicomponent interposed micropatterns of metal nanoparticles by sequential pulsed electrodepositions of different metals (e.g. Co, Ni) onto a prepatterned substrate (e.g. Al foil). The micropatterned cobalt and nickel nanoparticles thus produced were further demonstrated to be catalytically active for growth of multicomponent carbon nanotube micropatterns, in which different nanotubes are interposed in an intimate fashion. These results, together with the highly generic nature characteristic of the electrochemical and photopatterning methods for region-specific deposition of various metallic and nonmetallic (e.g. conducting polymers) species, indicate that the methodology developed in this study could be regarded as a general approach to the construction of multicomponent and multifunctional nanomaterials and nanodevices for a wide range of potential applications.

Acknowledgments

We are grateful for financial support from the NSF, ACS-PRF and Ohio State Government through the Wight Center of Innovation (WCI) Program. Thanks are due also to AFRL/ML, Wright Brothers Institute, Dayton Development Colations, and University of Dayton for a WBI Endowed Chair Professorship in Nanomaterials for LD.

References

- [1] Davydov D N A, Sattari P A, AlMawlawi D, Osika A, Haslett T L and Moskovits M 1999 *J. Appl. Phys.* **86** 3983
- [2] Lee Y-H, Choi C-H, Jang Y-T, Kim E-K and Ju B-K 2002 *Appl. Phys. Lett.* **81** 745
- [3] Merkulov V I, Lowndes D H, Wei Y Y, Eres G and Voelkl E 2000 *Appl. Phys. Lett.* **76** 3555
- [4] Bower C, Zhou O, Zhu W, Werder D J and Jin S H 2002 *Appl. Phys. Lett.* **77** 2767
- [5] Siegal M P, Overmyer D L and Provencio P P 2002 *Appl. Phys. Lett.* **80** 2171
- [6] Ducati C, Alexandrou I, Chhowalla M, Amaratunga G A J and Robertson J 2002 *J. Appl. Phys.* **92** 3299
- [7] Mayne M, Grobert N, Terrones M, Kamalakaran R, Ruhle M, Kroto H W and Walton D R M 2001 *Chem. Phys. Lett.* **338** 101
- [8] Kind H, Bonard J M, Emmenegger C, Nilsson L O, Hernadi K, Maillard-Schaller E, Schlappbach L, Forro L and Kern K 1999 *Adv. Mater.* **11** 1285
- [9] Colomer J F, Bister G, Willems I, Konya Z, Fonseca A, Van Tendeloo G and Nagy J B 1999 *Chem. Commun.* **14** 1343

- [10] Alvarez W E, Kitiyanan B, Borgna A and Resasco D E 2001 *Carbon* **39** 547
- [11] Matsumoto K, Kinoshita S, Gotoh Y, Uchiyama T, Manalis S and Quate C 2001 *Appl. Phys. Lett.* **78** 539
- [12] Cheung C L, Kurtz A, Park H and Lieber C M 2002 *J. Phys. Chem. B* **106** 2429
- [13] Li Y, Liu J, Wang Y Q and Wang Z L 2001 *Chem. Mater.* **13** 1008
- [14] Huang S M, Dai L M and Mau A W H 1999 *J. Phys. Chem. B* **103** 4223
- [15] Yang Y Y, Huang S M, He H Z, Mau A W H and Dai L M 1999 *J. Am. Chem. Soc.* **121** 10832
- [16] Li D C, Dai L M, Huang S M, Mau A W H and Wang Z L 2000 *Chem. Phys. Lett.* **316** 349
- [17] Endo M, Takeuchi K, Kobori K, Takahashi K, Kroto H W and Sarkar A 1995 *Carbon* **33** 873
- [18] Satishkumar B C, Govindaraj A and Rao C N R 1999 *Chem. Phys. Lett.* **307** 158
- [19] Andrews R, Jaques D, Rao A M, Derbyshire F, Qian D, Fan X, Dickey E C and Chen J 1999 *Chem. Phys. Lett.* **303** 467
- [20] Su M, Zheng B and Liu J 2000 *Chem. Phys. Lett.* **322** 321
- [21] Kukovec A, Konya Z, Nagaraju N, Willems I, Tamasi A, Fonseca A, Nagy J B and Kiricsi I 2000 *Phys. Chem. Chem. Phys.* **2** 3071
- [22] Chen Y, Wang Z L, Yin J S, Johnson P J and Prince R H 1997 *Chem. Phys. Lett.* **272** 178
- [23] Huang Z P, Wu J W, Ren Z F, Wang J H, Siegal M P and Provencio P N 1998 *Appl. Phys. Lett.* **73** 3845
- [24] Jeong S-H and Lee K-H 2003 *Synth. Met.* **139** 385
- [25] Lee J S and Suh J S 2002 *J. Appl. Phys.* **92** 7519
- [26] Tu Y, Huang Z P, Wang D Z, Wen J G and Ren Z F 2002 *Appl. Phys. Lett.* **80** 4018
- [27] Cai Z and Martin C R 1989 *J. Am. Chem. Soc.* **111** 4138
- [28] Harris P J F 2001 *Carbon Nanotubes and Related Structures—New Materials for the Twenty-First Century* (Cambridge: Cambridge University Press)
- [29] Dai L 2004 *Intelligent Macromolecules for Smart Devices: From Materials Synthesis to Device Applications* (New York: Springer)
- [30] Dai L, Patil A, Gong X, Guo Z, Liu L, Liu Y and Zhu D 2003 *Chem. Phys. Chem.* **4** 1151 and references cited therein
- [31] Yang Y, Huang S, He H, Mau A W H and Dai L 1999 *J. Am. Chem. Soc.* **121** 10832
- [32] Chen Q and Dai L 2000 *Appl. Phys. Lett.* **76** 2719
- [33] Yang J, Dai L and Vaia R A 2003 *J. Phys. Chem. B* **107** 12387
- [34] Kenneth B K, Teo K B K, Singh C, Chhowalla M and Milne W I 2003 *Encyclopedia of Nanoscience and Nanotechnology* vol X, ed H S Nalwa (California: American Scientific Publishers) p 1